In recent years, minimally invasive image-guided surgical procedures have grown both in popularity and sophistication. Ultrasound is an ideal imaging technology for such procedures from the perspective of cost, ease of use, and patient radiation exposure. However, ultrasound-guided procedures remain primarily manual, subject to the skill of a particular physician or ultrasound technician. And challenging issues exist in the use of ultrasound for image-guided procedures because of the physics of image acquisition and inaccuracies in calibration.

Intellectual Merit: This proposal seeks to develop advanced mathematical and computational methods for the online calibration of ultrasound probes that takes into account a probabilistic version of the well-known $AX = XB$ sensor-calibration problem that has been overlooked in the robotics and computer vision literature. In particular, rather than solving for a single position and orientation, X, we seek to characterize the probability density function $f_X(H)$ that takes as its argument rigid-body poses, H, and is peaked at X, but has a distribution around it. And using this distribution, rather than a single sample drawn from it, we seek to better reconstruct 3D environments from ultrasound image wedges, and to quantify tool positioning errors in ultrasound-guided surgical procedures. We also seek to perform automated online calibration in order to ensure that data collected during an ultrasound sweep is registered correctly. And we seek to construct optimal calibration moves so as to obtain the most accurate calibrations by reducing redundancy and deficiency. This new theory will be used in the context of an existing physical test setup consisting of a state-of-the-art 3D ultrasound probe and a selection of tissue-substitutes made of non-biological gel materials.

Solving the problem posed here will make ultrasound a more effective tool for guiding minimally invasive surgical procedures. Moreover, the classical $AX = XB$ problem has found applications in a wide variety of application areas including calibration of sensors in robotic wrists, cameras, atomic force microscopes, and, through the work of the co-PI, ultrasound probes. The new, probabilistic, version of the $AX = XB$ problem that we seek to solve in the context of ultrasound applications will result in a new methodology that will be equally applicable to all of the other areas listed above. Our methodology will draw from, and contribute to, the fields of probability theory, Lie groups, and noncommutative harmonic analysis, and will open up a new set of tools for use by applied researchers in need of improved calibration methods.

Broader Impact: The broader impact of this proposal comes in three forms:

(1) the techniques to be developed will lead to software that will advance current capabilities in computer-integrated surgical interventions, and will enable the PIs to generate preliminary data on phantom models to then pursue funding for applied clinical studies that will have tangible impact on the lives of people with cancer of the breast, prostate, liver, and kidney;

(2) This proposal brings together a theoretician/math modeler (the PI) and an applied researcher from the radiology department at Johns Hopkins Hospital (the co-PI). In addition to achieving the scientific aims, this effort will serve as an example for other collaborations between researchers in basic engineering science and researchers from the field of medicine (and in particular, interventional radiology);

(3) The Laboratory for Computational Sensing and Robotics (LCSR) at JHU has an established summer program for visiting undergraduate students that will facilitate involvement of undergraduates in the proposed research. In addition, the PI continues to mentor high school students from Baltimore Polytechnic High School through research experiences both during the academic year and the summer. The hands-on and visual nature of ultrasound image acquisition together with the mathematical problems of registration and calibration make this an ideal project to introduce students to the importance of mathematics.

Keywords: Ultrasound; Calibration; Lie Groups; Covariance Propagation; Image-Guidance

1 Introduction

We seek to develop a methodology for solving a probabilistic version of the classical $AX = XB$ sensor-calibration problem where X, A, B are all rigid-body motions/poses represented as homogeneous transformation matrices. We propose to apply this methodology to image-guided surgical planning, and particularly ultrasound-guided procedures. Whereas the classical $AX = XB$ problem is formulated to provide a single solution, "X", we seek to find a distribution of solutions, "$f_X(H)$," which is a probability density over the set of all rigid-body motions peaked at X, but with some distribution around it. That is,

$$f_X(H) \geq 0 \quad \text{and} \quad \int_{SE(3)} f_X(H)dH = 1 \quad \text{and} \quad \underset{H \in SE(3)}{\operatorname{argmax}} \; f_X(H) = X$$

where dH is the unique (up to scale) invariant integration measure, and $SE(3)$ is the 6D space of rigid-body motions/poses, called the "Special Euclidean" group of three-dimensional space. The benefit of this approach is that confidence intervals can be established and actions can be updated to either: (1) gather new information for re-calibration when the covariance of "$f_X(H)$" is too high; or (2) when the task involves reaching a target (as in image-guided therapy), actions can be performed to cover a region based on quantifiable descriptions of the uncertainty in tool pose.

This study will draw on and contribute to the full spectrum of research styles from theoretical to computational to experimental. The experimental part of our studies will not be performed on any humans or animals (live or dead), but will be performed on synthetic polymeric phantoms to validate the theory. And after the successful completion of this NSF basis research effort, we will explore more applied NIH clinical funding. We will also meet with representatives from companies who may be interested in using our methods, and seek to develop a consortium whereby all of these companies will have access to our methods. See letters of collaboration from Ultrasonics and Resonant Medical.

1.1 Motivation: Image-Guided Radiofrequency Ablation

Image-guided surgery (IGS) systems allow a surgeon to have more information available at the surgical site while performing a procedure, and as a result can be used to minimize the degree of invasiveness and trauma to the patient. This simultaneously reduces the cost, morbidity, and recovery time associated with a surgical procedure. Image acquisition for IGS can be achieved using different modalities such as fluoroscopy, computed tomography (CT), magnetic resonance imaging (MRI) or ultrasound (US). Of these, ultrasound is the sole imaging technology that is simultaneously hand held, produces no ionizing radiation (which is important both to the patient and to the surgeon), and imposes no requirements on the types of tools used in the imaging field (i.e., unlike MRI, the use of metal tools is okay). Moreover, US is very inexpensive both in terms of initial cost and long-term maintenance in comparison to other imaging technologies, and produces images at a comparatively rapid rate. The drawbacks of US are poorer image quality and the difficulty in accurate calibration and registration of images in order to effectively perform surgical interventions.

1.2 Relevance to Treating Liver Cancer

Ultrasound is particularly important in image-guided ablation of cancerous tumors of the liver. In spite of recent advances in cancer therapy, treatment of primary and metastatic tumors of the liver remains a significant challenge to the health care community worldwide. Hepatocellular

carcinoma (HCC) is one the most common malignancies encountered throughout the world (>1 million cases per year) and is being seen with increasing frequency in Western countries due to the changing prevalence of hepatitis C [1]. In the U.S. alone, 1 in 153 individuals will develop HCC with reported 5-year survival rates of less than 15 percent [2]. In addition, both prevalence and mortality rates for this disease particularly impact Hispanic and African American populations in the U.S. [3, 4]. Metastatic disease to the liver from a variety of primary malignancies is also a common health problem facing many in the U.S. and worldwide. Specifically, hepatic metastatic disease from colorectal cancer comprises the most commonly locally treated hepatic malignancy in the U.S. [5].

Whether for primary liver cancer or hepatic metastases, liver resection (partial hepatectomy) is the best option for potential cure in patients with confined disease. In selected cases of early HCC, total hepatectomy with liver transplantation may also be considered. Unfortunately, less than 25 percent of patients with primary or secondary liver cancer are candidates for resection or transplantation, primarily due to tumor type, location, or underlying liver disease. Moreover, many patients' tumors recur within the liver following resection, and few of these are candidates for re-resection. Consequently, increasing interest has been focused on ablative approaches for the treatment of unresectable liver tumors. Rather than extirpation, this technique uses complete local in situ tumor destruction. A variety of methods have been employed to locally ablate tissue. Radiofrequency ablation (RFA) is the most commonly used and perhaps most promising modality for tumor ablation [6, 7], but other techniques are also used, including ethanol injection, cryotherapy [8], irreversible electroporation [9] and microwave [10]. In all cases, ablation utilizes image guided placement of a probe within the target area in the liver parenchyma as shown in Figure 1 (where the US probe is shown at the top of the scene together with the small wedge within the scene that it can image). In RFA, heat created around an electrode is conducted into the surrounding tissue, causing coagulative necrosis at temperatures between 50 degrees C and 100 degrees C. In addition to increasing the number of patients eligible for curative therapy of liver cancer in unresectable patients, local tissue ablation has a significant advantage over resection in that it can be performed using a minimally invasive approach, including percutaneously and laparoscopically.

Recent evidence suggests thermal ablation in some cases can achieve results comparable to that of resection. Specifically, a recent randomized clinical trial comparing resection to RFA for small HCC found equivalent long-term outcomes with lower morbidity in the ablation arm [11, 12]. Several other studies have demonstrated the effectiveness of RFA for larger liver tumors, including those in excess of 4-5cm [13, 14]. Importantly, most studies suggest that efficacy of RFA is highly dependent on the experience and diligence of the treating physician, often associated with a steep learning curve [15]. Moreover, the apparent efficacy of open operative RFA over a percutaneous approach reported by some studies suggest that difficultly with targeting and imaging may be contributing factors [16]. Studies of the failure patterns following RFA similarly suggest that limitations in real-time imaging, targeting, monitoring of ablative therapy are likely contributing to increased risk of local recurrence [16]. Whether RFA should be considered comparable to resection remains controversial [17]. Yet, even in unresectable patients, the role for ablative therapy for liver can-

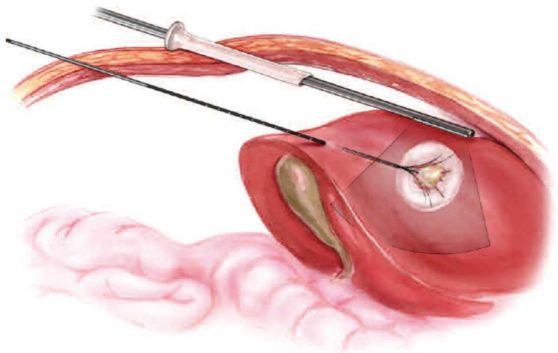

Figure 1: Laparoscopic radiofrequency ablation of a liver tumor guided by freehand 2D-US.

cer is potentially great. This approach often allows for greater preservation of uninvolved liver parenchyma, particularly in patients with cirrhosis or limited liver remnant volume (e.g. if combined with resection). In cases of liver metastases, tumors which are multiple, bilateral, or in areas not technically resectable are potentially well suited for this approach. In addition, RFA may be applicable for liver recurrence following prior liver resection, a situation in which long-term survival remains high but the morbidity of repeat hepatectomy may be high.

1.3 The Importance of Ultrasound Calibration

The critical importance of sensor calibration in IGS is illustrated in Figure 1 in which the surgical procedure is guided by an ultrasound probe.[1] Currently, ablation actions are taken based on the assumption that the ultrasound pose calibration is perfect. If there is uncertainty in this calibration, then the tumor will not be "cooked" in an optimal way, e.g., the ablator may not be positioned at the center of the tumor, or it may miss altogether. Quantifying uncertainty in calibration provides information with which to reposition an ablator and provides information about how far around a target region to ablate. And when the uncertainty is too high, covariance information can be used to indicate that re-calibration is necessary before taking any action.

2 INTELLECTUAL MERIT

2.1 Technical Formulation

In this section we explain: (1) how the $AX = XB$ arises in ultrasound; (2) review methods for solving this equation which date back a quarter century [18, 19, 20, 21], and continue to be refined and widely used in the calibration of various different kinds of sensors [22]-[32]; and (3) introduce our new probabilistic formulation that is motivated by ultrasound applications, but is also applicable to the full range of problems in which sensor calibration arises.

2.1.1 The $AX = XB$ Problem in Ultrasound

Significant previous research has been dedicated to quantitative tracked ultrasound which requires tracking the US probe in 3D space with respect to a stationary frame of reference. Tracking is typically achieved by rigidly attaching 3D localizers to the US probe. The spatial transformation between the US image pixels and the tracking body attached to the US probe must be evaluated through calibration process. Hence, calibration is ubiquitously present in all systems where ultrasound is used for quantitative image guidance. Accuracy of calibration is the most significant factor influencing the accuracy of externally tracked US systems and therefore it is a logical imperative to minimize calibration error.

The co-PI's current algorithms perform off-line US and tool (ablator device) calibration prior to interventional procedures, using well established calibration methods. Research in this area utilizes a closed-form formulation [33], which is now integrated in a calibration toolkit, called UltraCal, that was previously published in 2005 [34]. Figure 2 presents the coordinate systems for the mathematical formulation of the calibration problem. Figure 3 highlights one method of

[1] Two kinds of probes are on the market: 2D and 3D. A 2D probe is one that provides a single planar image wedge for each orientation of the probe; and a 3D probe is one that provides a spatial image wedge.

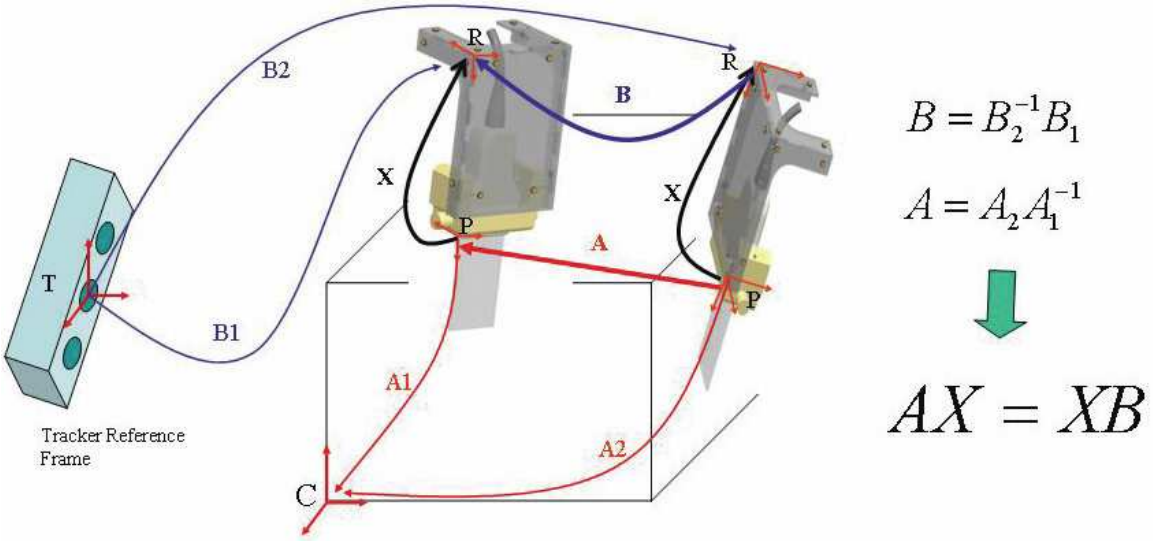

Figure 2: Defining Reference Frames for the $AX = XB$ Problem in Ultrasound

choosing C using a double-wedge phantom [35].[2] Here $I_{m(k)}$, $I_{m(k+1)}$ are the transformations of the US image coordinate system (P) with respect to the fixed reconstruction coordinate system (C) at poses k and k+1, respectively. The actual selection of C is arbitrary and the only requirement is that it must be rigidly fixed during the calibration process.

Using $I_{m(k)}$, $I_{m(k+1)}$, we can obtain the transformation between poses A_k and A_{k+1}, as A. Obviously, A can be estimated indirectly through recovering $I_{m(k)}$, $I_{m(k+1)}$ using a calibration phantom, or measured directly by matching 3D volumes acquired using a 3D US probe. B_k, B_{k+1} are the tracking device readings for the sensor frame (R) with respect to tracker reference frame (T) at poses k and k+1 respectively. The relative pose between sensor frame (R) at pose k and $k+1$ is given by $B = (B_{k+1})^{-1} B_k$. Figure 2 illustrates this for $k = 1$. This yields the homogeneous matrix equation

$$AX = XB \tag{1}$$

where A is estimated from planar images (or image volumes), B is assumed to be known from the external tracking device, and X is the unknown transformation between the US image coordinate system and the sensor frame (R) [35].

The vast majority of intraoperative hazardous situations in tracked US systems are caused by failure of registration between tracking and imaging coordinate frames, resulting in miscalibration of the tracked US. The most typical form of error is a false reading of the tracker. This occurs quite often in electromagnetic tracking systems due to invisible field distortions caused by metal objects or electromagnetic noise. Another typical problem related to tracking is deformation or physical damage of the tracking body attached to the probe, causing a latent misreading of pose. These problems are exceedingly dangerous because they occur without apparent warning. Among human operator errors, inadvertent changes in lateral image polarity occur quite frequently and transparently to the clinical user. Additionally, faulty conditions may arise from field distortion in the case of EM tracking or fluid/blood touching one of the LEDs and causing skewing of optical tracking measurements. Moreover, the speed of sound (SoS) changes considerably during

[2]This phantom consists of rigid metalic slots into which the US probe can be parked for the purpose of calibration. This is not to be confused with a polymeric phantom, which in our studies serves as a proxy for real patient tissues and has no such fiducial markers. The dual use of the word 'phantom' is an unfortunate quirk of the literature.

ablation, which affects the scale ratios and re-calibration is certainly needed. With regular offline recalibration some of the aforementioned errors can be caught prior to procedure. The process is called quality control (QC), and is a mandatory routine in any clinical department. Typically, QC is performed annually, monthly, or weekly, which places a heavy financial burden on the clinical department.

Annually, clinical centers guide millions of radiation therapy procedures using infrequent and expensive quality control protocols. Assuming an error rate of 0.1 percent this translates to thousands of sub-optimal radiation therapy delivery procedures. What is required therefore is a paradigm shift in calibration technology to a phantomless self-calibration that is performed directly on the patient, intraoperatively, in real-time, and transparently to the physician. One of the major incentives of our novel self-calibration work, in addition to increasing patient safety, is to reduce costs of QC and accelerating the use of US-guided intervention systems. Second, in addition to offline calibration, we will implement ultrasound self-calibration and QC methods to leverage the offline calibration and correct for SoS variations during thermal therapy. The two key enablers of our proposed self-calibration method is a closed-form mathematical formulation of the problem [33]. The co-PI has exploited this closed-form formulation to solve the calibration problem based on various mechanical phantoms including the double-wedge phantom [35], the N-shape phantom [33], and the thin wall phantom [36]. In all these methods, calibration phantoms were built in order to assist estimation of A's, which is the relative motion between successive US frames as shown in Figure 2. The current formulation of the calibration task reduces to recovering A's as we are scanning and collecting the corresponding B's from the tracker, and then using classical methods to obtain their calibration. Obviously, recovering A's from real-time US sequences is a problem of tracking rather than a problem of feature segmentation from static US phantom images. Tracking the 6 DOF of A's based on 3DUS data is considered a straightforward and easy to handle problem. What is missing, however, in current formulations is the quantification of error in the resulting calibration, which is the subject of this proposal.

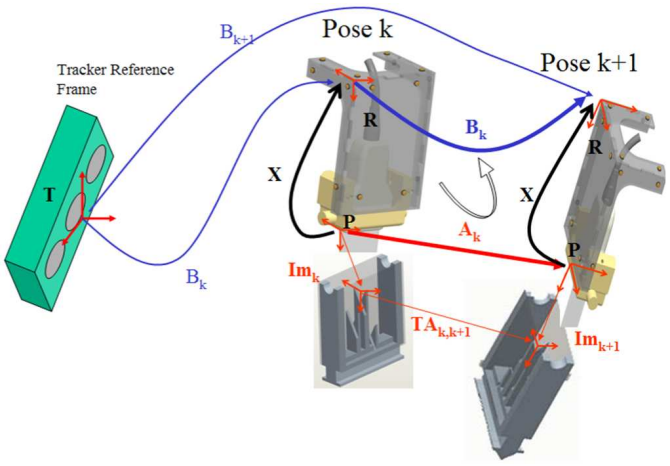

Figure 3: Calibration in Ultrasound Using a Tracker and Phantom Consisting of Rigid Slots at Known Poses

2.1.2 Classical Solutions to the $AX = XB$ Problem

Let $H(R, \mathbf{t})$ denote a 4×4 homogeneous transformations of the form

$$H(R, \mathbf{t}) = \begin{pmatrix} R & \mathbf{t} \\ \mathbf{0}^T & 1 \end{pmatrix}$$

where R is a 3×3 rotation matrix, and $\mathbf{t}$ is a translation vector. The set of all homogenous transformations together with the operation of matrix multiplication is well-known in robotics and computer vision as the group $SE(3)$, the "special Euclidean transformations of three-dimensional

space". The group operation, $\circ$, is simply multiplication of homogenous transformations gives

$$H(R_1, \mathbf{t}_1) \circ H(R_2, \mathbf{t}_2) = H(R_1 R_2, R_1 \mathbf{t}_2 + \mathbf{t}_1).$$

This operation can be suppressed to simplify notation, and so $H_1 \circ H_2$ can be abbreviated as $H_1 H_2$, though in some contexts it is useful to keep the $\circ$ for emphasis.

Every homogeneous transformation can be viewed as the matrix exponential of the form

$$H = \exp M \quad \text{where} \quad M = \begin{pmatrix} \Omega & \mathbf{v} \\ \mathbf{0}^T & 0 \end{pmatrix} \quad \text{where} \quad \Omega = -\Omega^T. \tag{2}$$

Associated with any 3×3 skew-symmetric matrix Ω is a dual vector $\boldsymbol{\omega} \in \mathbb{R}^3$ such that $\Omega \mathbf{x} = \boldsymbol{\omega} \times \mathbf{x}$ for every $\mathbf{x} \in \mathbb{R}^3$.

For almost all $H \in SE(3)$ it is possible to define an inverse (logarithm) to recover $(\Omega, \mathbf{v})$ from H. When the Frobenius norm of Ω is small in the sense that $\|\Omega\| << 1$, and when the vector 2-norm of $\mathbf{v}$ is small in the sense that $\|\mathbf{v}\| << 1$, then $R \approx \mathbb{I} + \Omega$ and $\mathbf{t} \approx \mathbf{v}$ where $\mathbb{I}$ is the 3×3 identity matrix. Here, $(\Omega, \mathbf{v})$ are not velocities, but rather are infinitesimal rigid-body motions (velocities multiplied by a small timestep, Δt). These quantities will be relevant in our probabilistic formulation in the next section. But first, we review the classical formulation.

The famous "$AX = XB$" problem in robot sensor calibration is stated as follows. Given a pair of measurements (A_i, B_i) where $A_i = H(R_{A_i}, \mathbf{t}_{A_i})$ and $B_i = H(R_{B_i}, \mathbf{t}_{B_i})$ for $i = 1, 2..., n$, find $X = H(R_X, \mathbf{t}_X)$ such that[3]

$$A_i X = X B_i \,. \tag{3}$$

Note that these n homogeneous-transform equations can only be solved exactly if the set of pairs $\{(A_i, B_i)\}$ for $i = 1, ..., n$ is compatible in the sense that a solution X exists. This is not always the case. The ways that compatibility can fail are: (a) At least one pair (A_i, B_i) is inconsistent in that no X can solve (3) for some fixed value of i; or (b) At least two pairs (A_1, B_1) and (A_2, B_2) cannot be solved by the same X; (c) Combinations of (a) and (b). As an example of (a), since from the above expression, $A_i = X B_i X^{-1}$, A_i and B_i must at least be similar matrices, and hence have all of the same eigenvalues, otherwise there cannot be a solution to (3). Note that searching for all $X \in SE(3)$ such that A_i and B_i are similarity-related for a fixed value of i is not sufficient to solve for X, since a continuum of solutions exist. As an example of (b), choose B_1 and B_2 at random from $SE(3)$. Then if for some choice of X_1, we can construct $A_1 = X_1 B_1 X_1^{-1}$, and for another choice $X_2 \neq X_1$, we can construct $A_2 = X_2 B_2 X_2^{-1}$. Then (3) will, by definition be solved individually for $i = 1$ and $i = 2$, but since $X_1 \neq X_2$, there is no mutual solution X in this scenario. Therefore, it would appear to only make sense to solve (3) for $i = 1, 2..., n$ when every pair (A_i, B_i) can result in a possible set of solutions, and these sets for $i = 1, 2..., n$ should have nonempty intersect. Even then, the set of pairs may be incomplete, in the sense that measurements are not varied enough to intersect at a single solution, $X \in SE(3)$. When this is the case, it is possible to use two pairs, say (A_i, B_i) for $i = 1, 2$, to obtain a solution. In cases when a single solution can be found, we can say that the set of pairs used is both compatible and complete.

Performing the matrix multiplication of homogeneous transformations in (1) and separating out the rotational and translational parts results in two equations of the form

$$R_A R_X = R_X R_B \tag{4}$$

[3]The A_i and B_i here are instances of the un-subscripted A and B in Figure 2 rather than the way subscripted poses are used in that figure, and are the same as the bold $\mathbf{A}_k$ and $\mathbf{B}_k$ in Figure 3 with $k = i$.

and

$$R_A \mathbf{t}_X + \mathbf{t}_A = R_X \mathbf{t}_B + \mathbf{t}_X. \tag{5}$$

The strategy to solve (1) would appear to reduce to first solving (4), and then rearranging (5) so as to find acceptable values of $\mathbf{t}_X$:

$$(R_A - \mathbb{I}_{3\times 3})\mathbf{t}_X = R_X \mathbf{t}_B - \mathbf{t}_A.$$

However, there are some problems with this naive approach. As pointed out in [19, 20, 21], there is a one-parameter set of solutions to (4), and the matrix $R_A - \mathbb{I}_{3\times 3}$ in general has rank 2. Hence, there are two unspecified degrees of freedom to the problem, and it cannot be solved uniquely unless additional measurements are taken.

This situation is rectified by considering two sets of exact measurements of the form in (1), i.e.,

$$A_1\, X = X\, B_1 \quad \text{and} \quad A_2\, X = X\, B_2$$

and using methods in [19, 20, 21], provided some mild conditions are observed for the selection of the pairs (A_1, B_1) and (A_2, B_2).

However, if there is sensor error, then it may not be possible to find compatible pairs that reproduce the exact value of X either due to (a), (b), or (c) failing. For this reason, minimization approaches are often taken where for $n > 2$ a cost function

$$C(X) = \sum_{i=1}^{n} w_i\, d^2(A_i X, X B_i) \tag{6}$$

is computed for some distance metric $d(\cdot, \cdot)$ on $SE(3)$ and $\{w_i\}$ is a set of weights which can be taken to be a partition of unity. A wide variety of such metrics are discussed in [37] that have the useful property of left-invariance, $d(H_0 H_1, H_0 H_2) = d(H_1, H_2)$ for any $H_0, H_1, H_2 \in SE(3)$. More recent work along these lines includes [38, 39, 40]. It is known that one can define either left-invariant or right-invariant metrics, but there are none that are simultaneously left and right invariant. Perhaps the simplest of the left-invariant ones is based on the weighted Frobenius norm

$$d^2(H_1, H_2) = \|H_1 - H_2\|_W^2 = \mathrm{trace}[(H_1 - H_2) W (H_1 - H_2)^T]$$

where W is a matrix that weights rotations and translations appropriately, as described in [37]. The sets of pairs (A_i, B_i) for $i = 1, 2..., n$ is chosen such that the set $\{A_i\}$ is spread out over a variety of positions and orientations, and likewise for $\{B_i\}$, so that the resulting X is robust to measurement errors.

Finding X that minimizes (6) is reasonable for obtaining a single consensus value that approximately solves (3), and a large literature on this exists [18, 19, 20, 21]. But this is not what we propose. We extend the problem in a new direction, and show how the PI's previous work on noncommutative harmonic analysis and covariance propagation are applicable. In particular, we seek to answer the question: Given a set of pairs of measurements, (A_i, B_i), where each A_i and B_i is drawn from a known error distributions (which can be reconstructed from a large number of measurements), how is this reflected in the distribution of error in X ? That is, rather than seeking a single consensus solution, we seek a distribution $f_X(H)$ with a corresponding mean and covariance that can be used to both quantify confidence in individual solutions and can be used directly to motionally average planar US images over 3D image volumes. Our approach is probabilistic and is described in the next section.

2.1.3 The Probabilistic $AX = XB$ Problem

Suppose that $\{(A_i, B_i)\}$ for $i = 1, ..., n$ is compatible and complete, in the sense that collectively they result in a unique solution to (3). Such would never be the case in true observations that are corrupted by noise. Rather, what would be presented are pairs $\{(A'^j_i, B'^j_i)\}$ for $i = 1, ..., n$ and $j = 1, ..., m_i$ where

$$A'^j_i = A_i \exp(M^j_i) \quad \text{and} \quad B'^j_i = B_i \exp(N^j_i)$$

where M^j_i and N^j_i are of the form of M in (2), and the components of these matrices are drawn from zero-mean probability density functions such as Gaussian distributions centered at zero, and with small covariances so that on average $\|M^j_i\|, \|N^j_i\| << 1$. These matrices represent the corruption of observations by small amounts of noise.

To put things in perspective, n might be a relatively small number like 3 or 10, whereas each m_i might be hundreds or thousands of measurements streaming from a sensor. And finding X that minimizes (6) with A'^j_i in place of A_i, B'^j_i in place of B_i, and an additional sum over j, will give a single valid estimate of the true underlying X. But if X is computed from a subset of these samples, then each time a slightly different value will be obtained. Therefore, when noise is present it makes more sense to talk about a distribution of values $f_X(H)$, and the solution to (6) with different subsets of measurements can be thought of as different samples drawn from $f_X(H)$.

In probability theory on $\mathbb{R}^n$, it is well known that the distribution of the sum of two random variables is the convolution of the probability densities of the individual random variables. An analogous situation results in the context of probability theory on Lie groups (of which $SE(3)$ is an example). This has been the subject of the PI's work for the past decade, and is summarized in [41]-[44]. The convolution of two probability densities on $SE(3)$ is

$$(f_1 * f_2)(H) = \int_{SE(3)} f_1(H') \cdot f_2(H'^{-1} \circ H) dH'$$

where $\cdot$ is scalar multiplication of functions, H' is a dummy variable of integration, and dH' is the bi-invariant integration measure for $SE(3)$. A common misconception is that the lack of a bi-invariant metric for $SE(3)$ implies the lack of a bi-invariant integration measure. This is not so. If the rotational part of H is parameterized by ZXZ Euler angles α, β, γ, the bi-invariant integration measure is (to within an arbitrary scaling constant) simply $dH = \sin\beta d\alpha d\beta d\gamma dt_1 dt_2 dt_3$. The criteria for an integration measure to be bi-invariant are less severe than for a metric to be.

This concept is applicable to ultrasound calibration as explained below. For each fixed i, given $\{A'^j_i\}$ and $\{B'^j_i\}$ with uncorrelated noises (since these come from independent sources: one comes from an optical tracker and the other comes from registering ultrasound images) it is possible to compute sample means and sample covariances $(\mu_{A_i}, \Sigma_{A_i})$ and $(\mu_{B_i}, \Sigma_{B_i})$. Here $\mu_{A_i}, \mu_{B_i} \in SE(3)$, and $\Sigma_{A_i}, \Sigma_{B_i} \in \mathbb{R}^{6\times 6}$ are symmetric covariance matrices. If the noise is small, or the number of samples is very large, $\mu_{A_i} \to A_i$ and $\mu_{B_i} \to B_i$. Explicitly, the sample mean can be defined as

$$\mu_{A_i} = \underset{\mu_{A_i} \in SE(3)}{\operatorname{argmin}} \left\| \sum_{j=1}^{m_i} \log\left(\mu_{A_i}^{-1} \circ A'^j_i\right) \right\|^2$$

where $\log(\cdot)$ is the inverse of the exponential in (2), and the sample covariance is

$$\Sigma_{A_i} = \frac{1}{m_i} \sum_{j=1}^{m_i} \log^\vee\left(\mu_{A_i}^{-1} \circ A'^j_i\right) \left[\log^\vee\left(\mu_{A_i}^{-1} \circ A'^j_i\right)\right]^T$$

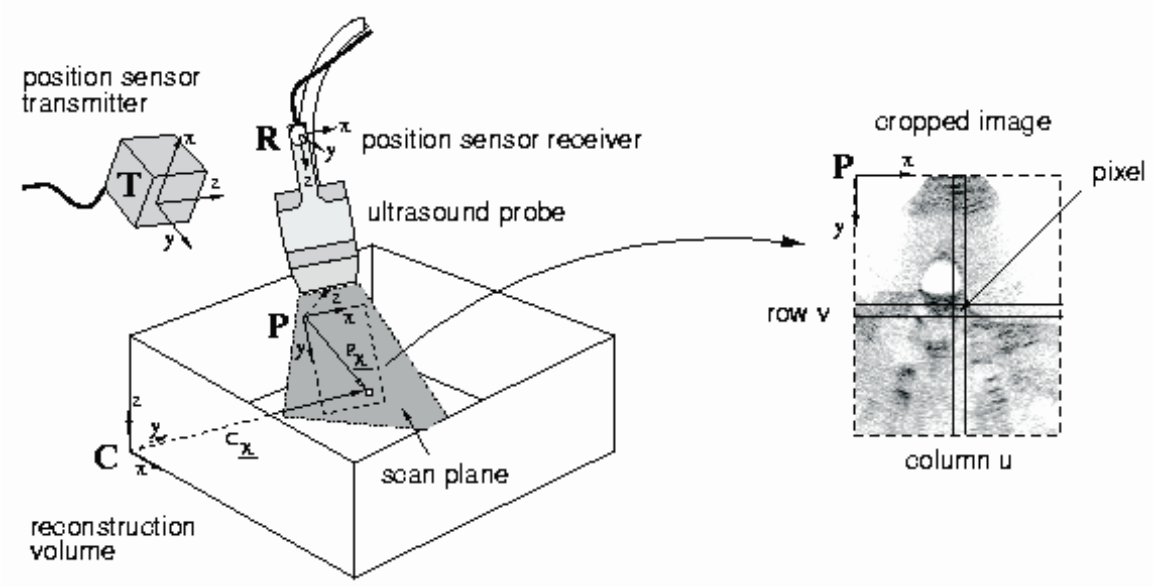

Figure 4: In Ultrasound Calibration The 'A' Has Undetermined Scale Factors (figure courtesy of Richard Prager)

(and similarly for B) where for any H expressed as in (2),

$$\log^{\vee}(H) = \begin{pmatrix} \boldsymbol{\omega} \\ \mathbf{v} \end{pmatrix}.$$

A Gaussian on $SE(3)$ can then be constructed as [44, 47]

$$f_{A_i}(H) = \frac{1}{(2\pi)^3 |\Sigma_{A_i}|^{\frac{1}{2}}} \exp\left\{ -\frac{1}{2} \log^{\vee}\left(\mu_{A_i}^{-1} \circ H\right) \Sigma_{A_i}^{-1} \left[\log^{\vee}\left(\mu_{A_i}^{-1} \circ H\right)\right]^T \right\}. \tag{7}$$

Using analogous definitions for $f_{B_i}(H)$ and $f_X(H)$, the probabilistic version of (6) that we will study is finding $f_X(H)$ (or, equivalently, (μ_X, Σ_X)) such that

$$\boxed{C(\mu_X, \Sigma_X) = \sum_{i=1}^{n} \int_{SE(3)} |(f_{A_i} * f_X)(H) - (f_X * f_{B_i})(H)|^2 \, dH} \tag{8}$$

is minimized. Unlike the case in (6) in which weights must be chosen, here the covariances Σ_{A_i} and Σ_{B_i} provide weights in a self-consistent and objective way. And taking the perspective that the solution is a probability density on $SE(3)$ rather than a single element $X \in SE(3)$ allows us to articulate and solve problems that previously were not even formulated. These are explained in the following section.

2.2 Proposed Work

We propose to solve the probabilistic version of the $AX = XB$ problem described as the minimization of (8) in several ways and in several variations as described in the goals below.

- Goal 1: Solve for the mean X and characterize the covariance/uncertainty in X when solving the noisy/probabilistic version of $AX = XB$ using intrinsic methods;

- Goal 2: Account for uncertainties in calibration and tracking when registering and reconstructing 3D image volumes;
- Goal 3: Apply these methods to interactive planning and online re-calibration in ultrasound-informed needle guidance.

Whereas the first goal is, in a sense, generic and applicable to vision systems, wrist sensors, and all of the other contexts in which the $AX = XB$ problem naturally arises, there is a special feature in the ultrasound problem related to goals 2 and 3 that adds an additional layer of difficulty, and hence makes it even more interesting. Namely, unlike in vision problems where light travels at the same speed through the atmosphere, in ultrasound imaging the waves travel through the tissue medium at a speed that depends on the medium. Assumptions are made about this speed in order to be able to interpret the resulting images, and the reconstruct the resulting 3D image blocks. A related problem is that the A_i's are not completely determined – there is an unknown scale factor in each of the component of translation that depends on the medium. That is, in addition to solving for X (or the distribution $f_X(H)$), we must also solve for these scale factors, which are a function of the US device, and in a given medium are independent of pose. That is, if $A_i = (R_{A_i}, \mathbf{t}_{A_i})$, then

$$\mathbf{t}_{A_i} = S\mathbf{u}_{A_i}$$

where $\mathbf{u}_{A_i} = (u, v, w)^T$ are coordinates as seen in an image wedge as depicted in Figure 4 and $S = \mathrm{diag}[s_1, s_2, s_3]$ is a diagonal matrix of unknown scale factors. Since S contains the same information as a 3D vector, $\mathbf{s}$, it is possible to write $S\mathbf{u}_{A_i} = D(\mathbf{u}_{A_i})\mathbf{s}$ where $D(\mathbf{u}_{A_i})$ is the diagonal matrix with diagonal entries of the form $D_{kk}(\mathbf{u}) = \mathbf{e}_k \cdot \mathbf{u}$.

As in the earlier figures, X in Figure 4 (though not labeled) is the pose of reference frame P relative to R. But this is measured indirectly by relating, on the one hand, features in the image to the space fixed-frame C, and on the other hand, the relationship between C, a tracker T, and R.

When the scaling issue is taken into account, the homogeneous transform equation $AX = XB$ still reduces to (4) and (5), but the latter becomes

$$R_A\mathbf{t}_X + D(\mathbf{u})\,\mathbf{s} = R_X\mathbf{t}_B + \mathbf{t}_X. \tag{9}$$

Co-PI Boctor came up with a method to solve this non-standard version of the $AX = XB$ problem based on (4) and (9) and multiple pairs (A_i, B_i). The core of this approach is to use the Kronecker product. Recall that If C is a matrix, $\mathrm{vec}(C)$ is the long vector produced by stacking the columns of C. If $\otimes$ denotes the Kronecker product, then

$$\mathrm{vec}(CDE) = (C \otimes E^T)\,\mathrm{vec}(D).$$

This means that (4) and (9) can be written together as [35]

$$\begin{bmatrix} \mathbb{I}_{9\times 9} - R_A \otimes R_b & \mathbb{O}_{9\times 3} & \mathbb{O}_{9\times 3} \\ \mathbb{I}_{3\times 3} \times \mathbf{t}_B^T & \mathbb{I}_{3\times 3} - R_A & -D(\mathbf{u}) \end{bmatrix} \begin{pmatrix} \mathrm{vec}(R_X) \\ \mathbf{t}_X \\ \mathbf{s} \end{pmatrix} = \mathbf{0}_{12} \tag{10}$$

where $\mathbb{I}_{m\times m}$ is the $m \times m$ identity, $\mathbb{O}_{m\times n}$ is the $m \times n$ zero matrix, and $\mathbf{0}_n$ is the n-dimensional zero vector.

By stacking multiple such equations for different pairs (A_i, B_i), linear constraint equations restrict the possible solutions, which exist in the null space of the matrix resulting from concatenated

the matrix on the left-hand-side of (10). This approach works very well in the case when there is no noise, but the effects of noise in the measurements of B_i and the part of A_i that is known may cause this method to break down in the sense that noise may cause the null space to be trivial, in which case no exact solution will be found. Therefore, we pursue an altogether different approach:

- Instead of taking and 'extrinsic' linear-algebraic approach in which the linearity of matrix equations are used to expand the dimension of the space to one which is 15 dimensional (nine entries of the rotation matrix R, three in the translation vector, and three in the scale vector) we will take an intrinsic geometric approach in which only the three degrees of rotational freedom of the rotation are treated in a coordinate-free manner, thus reducing the problem to nine dimensions. (part of Goal 1).
- We will handle the effects of noise intrinsically using a combination of covariance-propagation methods and noncommutative harmonic analysis. (part of Goal 1).
- We will apply these methods to online re-calibration of ultrasound probes and apply to needle-guided procedures (Goals 2 and 3).

The following subsections break down the problem into the case when A_i and B_i are both completely known, followed by the case when the scale factors are also unknown, and articulates the project goals more fully.

2.2.1 Goal 1: Solve for the Mean X and Characterize the Covariance/Uncertainty in X When Solving the Noisy $AX = XB$ Using Intrinsic Methods

This goal has three theoretical obectives:

(a) Compute X from (6) for sets of noisy measurements (A'^j_i, B'^j_i) for $i = 1, 2, ...n$ and $j = 1, ..., m_i$ for simulated and real ultrasound data and compare with the sample mean μ_X;

(b) Compute the residuals $\log^\vee(A'^j_i X (B'^j_i)^{-1} X^{-1})$, and compare with the resulting covariance Σ_X;

(c) Extend methods of multivariate statistical analysis from $\mathbb{R}^n$ to the context of $SE(3)$ data as needed to assess confidence in solutions to X from (6) and (μ_X, Σ_X) from (8).

These objectives will be pursued using two main approaches.

Our first approach to address this goal is to employ the concept of a Gaussian distribution as defined in (7), and using corresponding closed-form formulas for propagation the mean and covariance under convolution. The application of these methods, developed previously by the PI in [44], to compute the cost $C(\mu_X, \Sigma_X)$ efficiently is new.

Our second approach to address this goal is to compute this cost using concepts from noncommutative harmonic analysis, as described in the PI's book [41]. The reason why this approach is relevant is that the concept of Fourier transform for functions of group valued argument exists, and has the corresponding concept of convolution theorem. This means that, for example, if $\hat{f}(\lambda)$ is the group Fourier transform of of $f(H)$, then

$$\widehat{(f_{A_i} * f_X)}(\lambda) = \hat{f}_X(\lambda)\hat{f}_{A_i}(\lambda).$$

The Fourier transforms of functions on noncommutative[4] groups such as $SE(3)$ are matrices, which reflects the fact that convolution is also not commutative. An extension of Parseval's equality allows the conversion of an integral over $SE(3)$ to an integral over its dual (or Fourier) space,

[4]That is, $H_1 H_2 \neq H_2 H_1$.

$\widehat{SE(3)}$, which means that methods from numerical linear algebra can be employed to tackle the problem.

2.2.2 Goal 2: Account for Uncertainties in Calibration and Tracking When Registering and Reconstructing 3D Image Volumes

Consider a 3D volume of soft tissue composed of muscle, fat, and internal organs. Each bodily tissue has a distinctive signature in terms of how it reflects ultrasound waves. This can be described by a function $\rho(\mathbf{x})$ over the image volume. The goal of ultrasound (or any soft-tissue imaging technique) is to differentiate tissue types, which is related to assessing $\rho(\mathbf{x})$. The ability and limitations of ultrasound to capture this information can be modeled using the methods that we propose, and these abilities can be enhanced by solving associated inverse problems that are formulated here for the first time.

A standard 2D ultrasound probe has a particular profile relative to the reference frame attached to its handle. This profile can be taken as a window function, $w(\mathbf{x})$, that, for example, could be modeled as having value of unity over a volume in front of the probe, and zero otherwise. (In practice, $w(\mathbf{x})$ might have tails that decay gradually to zero, and the formulation here will be kept general).

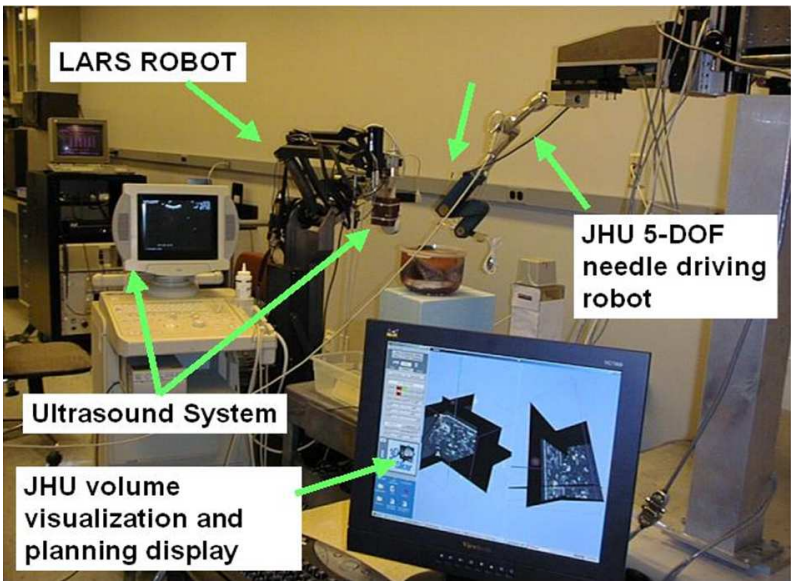

Figure 5: Current Hardware: Ultrasound Robot

The location of the 3D volume of interest (which would be inside of a patient laying on a table) will be registered to a 3D tracker fixed near the table. The handle of the ultrasound probe will be tracked. Since this will have some error associated with it, it can be described as $f_{T(t)}(H;t)$ where T stands for 'tracker' and t is time. This pdf may have different covariance and mean (which may be different from the true pose of the US probe handle) depending on where along the time-parameterized trajectory the handle is. Moreover, the position and orientation of the frame attached to the acquired US image relative to the handle is not known exactly, but rather is given by $f_X(H)$. And the process of image acqusition is not simply that of computing a slice, but rather is one of the form

$$i(\mathbf{x};H) = \int_{\mathbb{R}^3} w(H^{-1}\circ\mathbf{x})\rho(\mathbf{x})d\mathbf{x}$$

where $H^{-1}\circ\mathbf{x} = R^T(\mathbf{x}-\mathbf{t})$ when $H=(R,\mathbf{t})$. The notation $i(\mathbf{x};H)$ reflects that a different US image is obtained when the probe is at a different pose in contact with the surface of the volume.

Since the pose H is not known with absolute certainty due to the fact that $f_X(H)$ and $f_{T(t)}(H;t)$ are not Dirac delta functions concentrated at exact values of X and $T(t)$, this lack of certainty should be incorporated into an attempted reconstruction of $\rho(\mathbf{x})$. Namely, rather than simply

placing the ultrasound slice image slice $i(\mathbf{x}; H)$ at $H = T(t) \circ X$, we propose the probabilistic approach of smearing $i(\mathbf{x}; H)$ by the uncertainty in H. This is described as

$$s(\mathbf{x}; t) = \int_{SE(3)} (f_{T(t)} * f_X)(H) \cdot i(\mathbf{x}; H) dH.$$

The 3D volume reconstruction from these images, while more blurred than the traditional approach, accounts for the fact that the crisp and clear 2D images usually used in the reconstruction of 3D image volumes may be positioned and oriented in the wrong ways. And when such information is used in the future to drive a robotic system such as the one shown in Figure 5 with real patients, it will be important for the calibration to be precise, and for uncertainties to be quantifiable. This robotic system currently exists in the LCSR and will be used to demonstrate improvements resulting from our algorithms, as described in the following goal.

2.2.3 Goal 3: Interactive Planning and Online Re-Calibration in Ultrasound-Informed Needle Guidance

Pre-operative image volumes such as CT and/or MRI are used as part of current surgical planning procedures. During an actual US-guided surgical procedure, it is useful to register the ultrasound volume to this pre-operative image volume, thereby providing the surgeon a sense of where to move the surgical tool. In minimally invasive procedures, the tool may be nothing more than a needle. A relatively rigid (18-20 gauge) needle will show up in an ultrasound image either as a straight edge or a point (representing the needle itself from different angles) as well as the shadow of the needle.

Currently in co-PI Boctor's lab pod (which is located within 15 meters walking distance from the PI's lab pod) in the Laboratory for Computational Sensing and Robotics (LCSR), an ultrasound system is set up. This is often used in conjuction with LARS and needle-insertion robots that are available for our use in the LCSR shared space. The whole existing setup that we will use to perform our experiments is shown in Figure 5. And Figure 6 shows the sorts of 3D image blocks that can be viewed with the image slicer system that we also have in house.

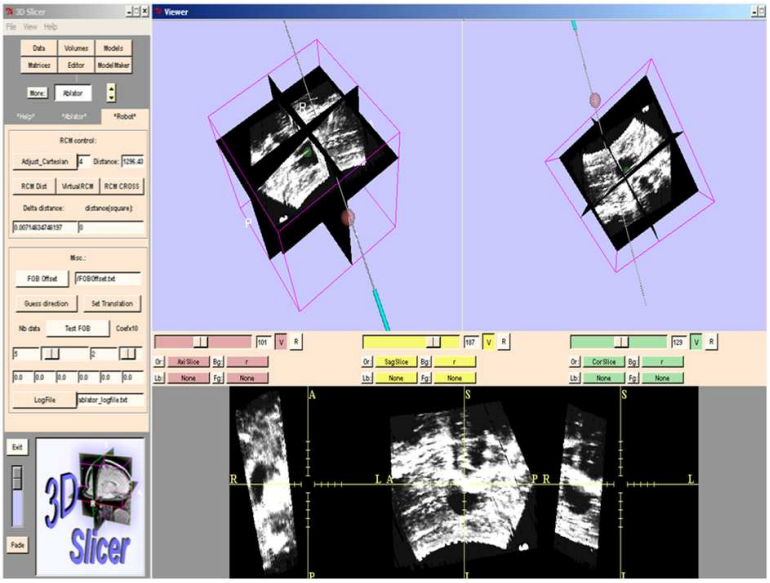

Figure 6: Ultrasound Slicer

We propose to use the needle itself as a fiducial, and to develop methods for automatically updating the pose of the US probe so as to gain the most information about the needle location relative to features in the pre-operative image volume. This requires that the registration of the US image and the calibration of the US probe pose must be robust to disturbances. Such disturbances can result from electromagnetic interference (metalic objects being placed in the electromagetic field, or occlusion of optical tracker). By continual online computation of $\tilde{f}_X(H; t)$, which denotes an

online version of $f_X(H)$, and comparison of these two distributions, provides a means to assess whether the tool becomes decalibrated.

2.3 Summary of Intellectual Merit

A probabilistic version of the sensor calibration problem is formulated here. This problem is of critical importance in improving the capabilities of ultrasound for image-guided minimally invasive surgical procedures. In the current state of the art where deterministic versions of the $AX = XB$ problem are solved, the range of potential errors in sensor calibration are not quantified. And therefore, in the context of current image guided procedures, one can be "far off the mark" without knowing it. Our solution method, which formulates the problem as a convolution equation over the group of rigid-body motions, utilizes the PI's expertise on this subject, and addresses a pressing need in medical robotics, the applied side of which is the subject of the co-PI's work. In addition to improving manual ultrasound-guided procedures by quantifying the range of possible pose errors in a given calibration, the method proposed here can be used in an iterative fashion to re-calibrate during image-guided surgical procedures. Moreover, in the many applications outside of ultrasound where the $AX = XB$ problem arises, our new probabilistic version of the problem can be used to quantify uncertainties before sensor data is interpreted and actions based on unquantified calibration errors are taken.

3 BROADER IMPACT

Our team (which consists of an engineer/mathematician and computer scientist/radiologist) can serve as a role model for interdisciplinary collaboration. As such, students with whom we interact at all levels (graduate, undergraduate, and student interns from local high schools and colleges) will be exposed to new ideas that combine theory, computation, and practical medical applications.

In addition to international scientific impact and interdisciplinary training of our students, we will also have impact on the local community in Baltimore City, as explained in the letter provided in supplemental material from Baltimore Polytechnic High School (a Baltimore City public school). Students from Baltimore Poly will spend several afternoons in his lab every week during the academic year through Poly's Research Practicum Program. Three former Poly students (Ms. Laura Carson and Mr. Burnest Griffin) who worked in the PI's lab in the past matriculated as undergraduates at JHU with full tuition waivers, via the Baltimore Scholars Program. And two others, Mr. Andrew Cushing and Ms. Princess Allen attended well-respected engineering schools under prestigious scholarships after spending their senior year of high school in the PI's lab. A number of others have gone on to pursue degrees at other prestigious colleges. Hence a template for success exists.

In addition, the Laboratory for Computational Sensing and Robotics (LCSR) at JHU has an established summer program for undergraduate students who visit from other universities which will further facilitate involvement of undergraduates in the proposed research. Both the PI and co-PI participate in this program by hosting students in their labs. Such students are particularly drawn to JHU for medical robotics. Moreover, in a typical year the PI hosts between three and five JHU undergraduates who become interested in his work through classess. Such students perform a combination of computer programming, mechatronics-based design, and mechanical construction. More details of their involvement in this project and their management are discussed in the Collaboration Plan section of this proposal.

3.1 Schedule

Though the PI and co-PI have appointments in different departments, they each have a lab pod on the same floor in the Laboratory for Computational Sensing and Robotics (LCSR), located 15 meters from each other. Therefore, it will be easy to establish monthly meetings with our students to monitor progress and keep on track with our objectives, as described in the Collaboration Plan. In addition to the technical objectives listed below for each year of the project, we will take on undergraduates and high-school students as described above. The schedule of activities for our effort are organized as follows:

- **Year 1:** We will write computer programs that implement Goal 1 in Section 2.2.1. That is, we will code up the the probabilistic sensor calibration problem described in Section 2.1.3 using the covariance propagation and Fourier methods described in Section 2.2.1.
- **Year 2:** We will solve Goal 2 described in Section 2.2.2, which is to account for uncertainties in calibration and tracking when registering and reconstructing 3D image volumes. This will be done first in computer simulation, and then on the existing physical phantom in the co-PI's lab.
- **Year 3:** We will solve Goal 3 described in Section 2.2.3, which is interactive planning and online re-calibration in ultrasound-informed needle guidance. This will involve sticking needles into the synthetic polymeric tissue phantom and reconstructing in 3D the needle location. This will build on the PI's prior collaborative work on flexible needle steering [46, 47, 48] which did not use ultrasound guidance. The current effort will use both rigid and flexible needles.
- **Year 4:** We will benchmark our software, write the final papers for the project, comment and release our code, and develop an industrial consortium for the dissemination of our results into practice (starting with the industrial collaborators described in the enclosed supporting letters). We will also line up clinical collaborators to take this effort to the next level, which in follow-on work will go beyond the synthetic polymeric phantoms that we use in this project.

3.2 PI's Relevant Prior Work

Dr. Greg Chirikjian (the PI), Professor of Mechanical Engineering, has been on the faculty at Johns Hopkins University since 1992. He is the author of more than 200 published works in the areas of robotics, DNA mechanics, elastic network models of proteins, image processing, and applied mathematics. Prior NSF and NIH funding has supported 17 PhD dissertations completed under the PI's sole guidance, and more than half of these graduates hold academic positions at institutions around the world. He currently has one small robotics project, NSF RI: "Robotic Inspection, Diagnosis and Repair" IIS-0915542 $ 369,000, 7/1/09-6/30/12, which supports 1.5 students. This is unrelated to the current proposal and has resulted in a number of publications so far [52]-[59]. And though the PI's current funded work is not in the medical area, in the past he has been involved in the analysis of a number of medical devices and imaging modalities including active cannulas [45], steerable needles [46, 47, 48], brachytherapy [49], and fiducial design for improved 3D image reconstruction [50, 51] under NIH funding and JHU's CISST ERC directed by Prof. Russ Taylor, which successfully completed its NSF funded phase several years ago. The co-PI, Dr. Emad M. Boctor, has not had independent NSF funding as a faculty member, but was supported JHU's CISST ERC during his graduate studies with Dr. Gabor Fichtinger.

4 Collaboration Plan

This plan reviews aspects of the PI and co-PI's backgrounds and their research groups that will facilitate collaboration, and explains the activities that we will engage in to enhance our collaboration.

4.1 Description of Personnel

Our team consists of the PI, Gregory Chirikjian, Professor of Mechanical Engineering, and the co-PI, Emad M. Boctor, Assistant Professor of Radiology, and their students. All participants are at Johns Hopkins University, and both the PI and co-PI have secondary appointments in the CS department.

The PI and all of the students have their offices in the Laboratory for Computational Sensing and Robotics (LCSR) on the JHU Homewood Campus. The co-PI, whose primary appointment is in the the School of Medicine (SOM) on the East Baltimore campus, maintains an office in the LCSR which is shared with other research faculty. The co-PI spends two days per week in the LCSR, where he has a lab pod to do his non-clinical work. (See facilities description of the layout of the LCSR. Both the PI and co-PI have lab pods on the same floor of this building, literally within 15 meters walking distance from each other). The PI and co-PI will meet once per month informally to touch base, and the whole team will meet quarterly, as discussed in more detail below under "Mentoring Activities."

One of the students in the project (Mr. Martin Kendal Ackerman) is a third-year PhD student working under the supervision of the PI. Mr. Ackerman is finished with coursework and teaching-assistant responsibilies, and will focus 100 percent on research. He is interested in becoming a professor, and performing research on this project will provide valuable experience to him, both in terms of developing his research skills, as well as teaching him about the teamwork aspects of collaborative research projects. The second student on the project will be an Master-of-Science student. In recent years, JHU, like many universities, has dramatically increased in the size of its student body pursuing Master of Science degrees. Students who previously would have been drawn into PhD programs are now lured into MSE (Master of Science in Engineering) or MSEM (Master of Science in Engineering Management) programs. Students from both programs henceforth will be referred to as 'MS students'. Such students usually take 1.5 years to finish, and after the first academic year of studies become interested in doing research. We have therefore budgeted for one PhD student (Mr. Martin K. Ackerman) and one MS student (yet to be determined) under the reasoning that the advanced mathematics in our formulation would be appropriate for a PhD student, and the applied experimental and data acquisition work would be suitable for an MS student. Turn-Over and Recrutment of New Graduate Students In the event that this proposal is funded, the first order of managerial business will be to advertise the MS position. Given the vast pool of MS students that currently exists, and the fact that many pay their own way while taking courses, we are confident that there will be many eager candidates for the MS position. These students are quite talented, and from the summer after their first academic year they will have the skills necessary to perform the experimental measurements in the project. In practice, whereas the PhD student will be involved for the first 2-3 years of the project before graduating, and turning his position over to another PhD student, the MS students will cycle through at a much faster rate (perhaps one per year, or even three every two years). This plan has pedagogical value, as future leaders in the technology-based industries and business leaders should have some understanding of the issues and processes involved in basic research, and some appreciation for its value.

Altogether we expect to train between six and ten students (two at any given time) over the

duration of the projection. Our whole team at any particular instant in time (the four individuals to be funded under this project: PI, co-PI, PhD student, MS student) will have regular monthly meetings to review project objectives and progress. In addition, an annual retreat (as described at the end of this plan) will be held which will make our results known to a wider collection of researchers.

4.2 Mentoring Activities Tailored to Graduate Students

A common problem in the modern sciences is that after completing their graduate studies, newly minted PhDs cycle through a series of postdoctoral positions, and never obtain a permanent faculty position or other position of leadership. The PI has had success in mentoring PhD students. Of those who have completed their PhD's under his supervision, 7 currently hold academic positions, and 3 others hold positions of leadership in their organizations. The best indicator of future success in mentoring is the success of previous apprentices. There are three elements to the PI's past success that will be replicated here:

- During each year for which the student is funded on this project, (s)he will present a paper at a large meeting such as ICRA, IROS, or MICCAI to gain exposure to his work, experience in public speaking, and making contacts for future job prospects.
- Each student must meet with his/her supervisors at least once per week, and present results to the whole team once every quarter as a formal seminar. During weekly meetings, career options will be discussed. During both weekly and quarterly meetings the fundamentals of the scientific method, laboratory safety, and other standards of professional practice will be discussed.
- Each student will be required to produce at least one archival journal article per year on which (s)he is primary author, and will assist the other student in the preparation of their manuscripts, and serve as a co-author on those. These will be written with the knowledge of ethics obtained from mandatory ethics classes (which also cover IP issues) that our institutions require of all students and postdocs engaged in research.

These common-sense rules are particularly powerful in aiding the students in an interdisciplinary team such as ours because: (1) individuals who can claim to have had exposure or training in both "medicine" and "engineering" are marketable both in academia and industry, thereby opening up a wider range of possibilities; (2) peer pressure plays a role in the sense that a history of success by current and past lab members establishes expectations of success and pushes current members to actively pursue job listings posted in professional magazines, online bulletin boards, and mass emails rather than taking a passive approach. In addition, the graduate students will be encouraged to join or maintain membership in one or more professional societies of his/her choosing; (3) by effectively screening and identifying the candidate in advance, the candidate is guaranteed to be a self-starter requiring very little time to come up to speed on the proposed project.

4.3 The Role of Undergraduates and High School Students

Each year the PI and co-PI host numerous undergraduate and high-school students in their labs. The Laboratory for Computational Sensing and Robotics (LCSR) has an established REU Program that the PI and co-PI have both participated in. Moreover, multiple undergraduates work in the PI and co-PI's labs during the school year, and during the summer. High school students will also be involved in our activities. (See letter of collaboration from Baltimore Polytechnic High School

and the Broader Impact section of the proposal). We have an established hierarchy in which each PI/co-PI manages graduates students via regular weekly meetings, and these graduate students in turn supervise undergraduate students and high school students.

4.4 Annual Retreat

In addition to the activities described above, we will have an annual retreat in which the participants will present their recent work, either in preparation for conferences such as ICRA, IROS, MICCAI, or as a repetition of their presentations at these conferences. During these retreats the full participation of both the PI's and co-PI's research groups (i.e., not only the students directly involved in this project) will be encouraged by the presence of free food, paid for by the PI's discretionary funds. Moreover, our industrial collaborators (see letters of collaboration) will be invited to learn about our developments, observe physical demonstrations, and interact with students. This will provide an opportunity for students to gain exposure and potential contacts for future employment.

References

[1] El-Serag HB, Davila JA, Petersen NJ, McGlynn KA. The continuing increase in the incidence of hepatocellular carcinoma in the United States: an update. Ann Intern Med. 2003 Nov 18;139(10):817-23.

[2] National Cancer Institute (NCI), Surveillance Epidemiology and End Results (SEER) providing information on cancer statistics on the U.S. population.

[3] Davila JA, El-Serag HB. Racial differences in survival of hepatocellular carcinoma in the United States: a population-based study. Clin Gastroenterol Hepatol. 2006 Jan;4(1):104-10.

[4] Sonnenday CJ, Dimick JB, Schulick RD, Choti MA. Racial and geographic disparities in the utilization of surgical therapy for hepatocellular carcinoma.J Gastrointest Surg. 2007 Dec;11(12):1636-46.

[5] Pawlik TM, Choti MA. Surgical therapy for colorectal metastases to the liver. J Gastrointest Surg. 2007 Aug;11(8):1057-77.

[6] Choti MA, "Hepatic radiofrequency ablation," The Cancer Journal 2000; 6(4): 291-2.

[7] Choti MA, "Surgical management of hepatocellular carcinoma: resection and ablation," J Vasc Interv Radiol. 2002 Sep;13(9 Suppl):S197-203.

[8] Kuszyk BS, Boitnott JK, Choti MA, Bluemke DA, Sheth S, Magee CA, Horton KM, Eng J, Fishman EK, "Local tumor recurrence following hepatic cryoablation: radiologic-histopathologic correlation in a rabbit model," Radiology. 2000 Nov;217(2):477-86.

[9] Rubinsky B, Onik G, Mikus P. Irreversible electroporation: a new ablation modality–clinical implications. Technol Cancer Res Treat. 2007 Feb;6(1):37-48.

[10] Zhang X, Zhou L, Chen B, Hu S, Wachtel MS, Frezza EE. Microwave ablation with cooled-tip electrode for liver cancer: an analysis of 160 cases. Minim Invasive Ther Allied Technol. 2008;17(5):303-7.

[11] Chen MH, Yang W, Yan K et al, Large liver tumors: protocol for radiofrequency ablation and its clinical application in 110 patients' mathematical model, overlapping mode, and electrode placement process, Radiology 232(1), 260-271 (2004).

[12] Chen MS, Li JQ, Zheng Y, Guo RP, Liang HH, Zhang YQ, Lin XJ, Lau WY. A prospective randomized trial comparing percutaneous local ablative therapy and partial hepatectomy for small hepatocellular carcinoma. Ann Surg. 2006 Mar;243(3):321-8.

[13] Gillams AR, Lees WR. Five-year survival following radiofrequency ablation of small, solitary, hepatic colorectal metastases. J Vasc Interv Radiol. 2008 May;19(5):712-7.

[14] Seror O, N'Kontchou G, Ibraheem M, et al. Large (¿or=5.0-cm) HCCs: multipolar RF ablation with three internally cooled bipolar electrodes–initial experience in 26 patients. Radiology. 2008 Jul;248(1):288-96.

[15] Poon RT, Ng KK, Lam CM, Ai V, Yuen J, Fan ST, Wong J. Learning curve for radiofrequency ablation of liver tumors: prospective analysis of initial 100 patients in a tertiary institution. Ann Surg. 2004 Apr;239(4):441-9.

[16] Mulier S, Ni Y, Jamart J, Ruers T, Marchal G, Michel L. Local recurrence after hepatic radiofrequency coagulation: multivariate meta-analysis and review of contributing factors. Ann Surg. 2005 Aug;242(2):158-71.

[17] Mulier S, Ni Y, Jamart J, Michel L, Marchal G, Ruers T. Radiofrequency ablation versus resection for resectable colorectal liver metastases: time for a randomized trial? Ann Surg Oncol. 2008 Jan;15(1):144-57.

[18] Arun, K.S., Huang, T.S., Blostein, S.D., "Least-Squares Fitting of Two 3-D Point Sets," *IEEE Trans. on Pattern Analysis and Machine Intelligence*, Vol. 9, No. 5, pp. 698-700, Sept. 1987.

[19] Chou, J.C.K., Kamel, M., "Finding the Position and Orientation of a Sensor on a Robot Manipulator Using Quaternions," *The International Journal of Robotics Research*, Vol. 10, No. 3, pp. 240-254, June 1991.

[20] Park, F.C., Martin, B.J., "Robot Sensor Calibration: Solving $AX = XB$ on the Euclidean Group," *IEEE Trans. Robotics and Automation*, Vol. 10, No. 5, pp. 717-721, Oct. 1994.

[21] Shiu, Y.C., Ahmad, S., "Calibration of Wrist-Mounted Robotic Sensors by Solving Homogeneous Transform Equations of the Form $AX = XB$," *IEEE Trans. Robotics and Automation*, Vol. 5, No. 1, pp. 16-29, Feb. 1989.

[22] Shaoping Bai and Ming Yeong Teo, "Kinematic Calibration and Pose Measurement of a Medical Parallel Manipulator by Optical Position Sensors," Journal of Robotic Systems 20(4), 201209 (2003)

[23] Irene Fassi, Giovanni Legnani, "Hand to Sensor Calibration: A Geometrical Interpretation of the Matrix Equation AX=XB," Journal of Robotic Systems 22(9), 497506 (2005)

[24] Motilal Agrawal, "A Lie Algebraic Approach for Consistent Pose Registration for General Euclidean Motion," Proceedings of the 2006 IEEE/RSJ International Conference on Intelligent Robots and Systems October 9 - 15, 2006, Beijing, China pp. 1891-1897.

[25] Klaus H. Strobl and Gerd Hirzinger, "Optimal Hand-Eye Calibration," Proceedings of the 2006 IEEE/RSJ International Conference on Intelligent Robots and Systems October 9 - 15, 2006, Beijing, China pp. 4647-4653

[26] Joseph Lam, Michael Greenspan, "An Iterative Algebraic Approach to TCF Matrix Estimation," Proceedings of the 2007 IEEE/RSJ International Conference on Intelligent Robots and Systems San Diego, CA, USA, Oct 29 - Nov 2, 2007 pp. 3848-3853

[27] Andreas Jordt, Nils T Siebel, and Gerald Sommer, "Automatic High-Precision Self-Calibration of Camera-Robot Systems," 2009 IEEE International Conference on Robotics and Automation Kobe International Conference Center Kobe, Japan, May 12-17, 2009 pp. 1244-1249.

[28] Yongduek Seo, Young-Ju Choi, Sang Wook Lee "A Branch-and-Bound Algorithm for Globally Optimal Calibration of a Camera-and-Rotation-Sensor System," 2009 IEEE 12th International Conference on Computer Vision (ICCV) pp. 1173-1178.

[29] Wei Dong, David Rostoucher, Michaël Gauthier, "Kinematics Parameters Estimation for an AFM/Robot Integrated Micro-Force Measurement System," The 2010 IEEE/RSJ International

Conference on Intelligent Robots and Systems October 18-22, 2010, Taipei, Taiwan pp. 6143-6148.

[30] Sin-Jung Kim, Mun-Ho Jeong, Joong-Jae Lee, Ji-Yong Lee, Kang-Geon Kim, Bum-Jae You, and Sang-Rok Oh, "Robot Head-Eye Calibration Using the Minimum Variance Method," Proceedings of the 2010 IEEE International Conference on Robotics and Biomimetics December 14-18, 2010, Tianjin, China pp. 1446 - 1451.

[31] Konstantinos Daniilidis, "Hand-Eye Calibration Using Dual Quaternions," The International Journal of Robotics Research 1999 18: 286-298.

[32] Yuchao Dai1, Jochen Trumpf, Hongdong Li, Nick Barnes, and Richard Hartley, "Rotation Averaging with Application to Camera-Rig Calibration," H. Zha, R.-i. Taniguchi, and S. Maybank (Eds.): ACCV 2009, Part II, LNCS 5995, pp. 335346, 2010.

[33] Boctor EM, Viswanathan A, Choti MA, Taylor RH, Fichtinger G, Hager GD, "A Novel Closed Form Solution for Ultrasound Calibration," In IEEE Int Symp. On Biomedical Imaging, 2004, pp. 527-530.

[34] Kon R, Leven J, Kothapalli K, Boctor EM et al.,"CIS-UltraCal: an open-source ultrasound calibration toolkit," Proc. SPIE, Vol. 5750, 516 (2005).

[35] Boctor EM, "Enabling Technologies For Ultrasound Imaging In Computer-Assisted Intervention," 2006, Computer Science Department, Johns Hopkins University.Thesis.

[36] Viswanathan A, Boctor EM, Taylor RH, Hager GD, Fichtinger G, Immediate Ultrasound Calibration from Two Poses and Minimal Image Processing, Seventh International Conference on Medical Image Computing and Computer-Assisted Intervention – MICCAI 2004, Proceedings in Lecture Notes in Computer Science Vol. 3217, pp 446-454, Springer, 2004.

[37] Chirikjian, G.S., Zhou, S., "Metrics on Motion and Deformation of Solid Models," *ASME J. Mechanical Design*, Vol. 120, No. 2, June, 1998, pp. 252-261.

[38] J. J. Kuffner, "Effective sampling and distance metrics for 3D rigid body path planning," *Proceedings of the 2004 IEEE ICRA*, pp. 3993 - 3998, 2004.

[39] Eberharter, J.K., Ravani, B., "Local Metrics for Rigid Body Displacements," ASME J. Mechanical Des. 126(5) September 2004 (8 pages) doi:10.1115/1.1767816

[40] Venkataramanujam, V., Larochelle, P.M., "A Coordinate Frame Useful for Rigid-Body Displacement Metrics," *ASME Journal of Mechanisms and Robotics*, Vol. 2, paper 044503 (5 pages), November 2010.

[41] Chirikjian, G.S., Kyatkin, A.B., *Engineering Applications of Noncommutative Harmonic Analysis*, CRC Press, Boca Raton, FL 2001.

[42] Chirikjian, G.S., Kyatkin, A.B.,"An Operational Calculus for the Euclidean Motion Group with Applications in Robotics and Polymer Science," *J. Fourier Analysis and Applications*, 6: (6) 583-606, December 2000.

[43] Chirikjian, G.S., *Stochastic Models, Information Theory, and Lie Groups*, Birkhäuser, 2009.

[44] Wang, Y., Chirikjian, G.S., "Nonparametric Second-Order Theory of Error Propagation on the Euclidean Group," *International Journal of Robotics Research*, Vol. 27, No. 1112, November/December 2008, pp. 12581273

[45] Rucker, D.C., Webster, R.J. III, Chirikjian, G.S., Cowan, N.J., "Equilibrium Conformations of Concentric-Tube Continuum Robots," *International Journal of Robotics Research*, vol. 29 no. 10 1263-1280, 2010.

[46] Cowan, N.J., Goldberg, K., Chirikjian, G.S., Fichtinger, G., Alterovitz, R., Reed, K.B., Kallem, V., Park, W., Misra, S., Okamura, A.M., "Robotic Needle Steering: Design, Modeling, Planning, and Image Guidance," in *Surgical Robotics – Systems, Applications, and Visions*, (J. Rosen, B. Hannaford and R. Satava, eds.), pp. 557–582, Springer, 2011,

[47] Park, W., Wang, Y., Chirikjian, G.S., "The path-of-probability algorithm for steering and feedback control of flexible needles," *International Journal of Robotics Research*, Vol. 29, No. 7, 813-830 (2010)

[48] Webster, R.J., III, Kim, J.-S., Cowan, N.J., Chirikjian, G.S., Okamura, A.M., "Nonholonomic Modeling of Needle Steering," *International Journal of Robotics Research*, Vol. 25, No. 5-6, May-June 2006, pp. 509-525.

[49] Jain, A., Zhou, Y., Mustufa, T., Burdette, E.C., Chirikjian, G.S., Fichtinger, G., "Matching and Reconstruction of Brachytherapy Seeds using the Hungarian Algorithm (MARSHAL)," *Medical Physics* 32 (11): 3475-3492 Nov 2005

[50] Jain, A., Mustafa, T., Zhou, Y., Burdette, E.C ., Chirikjian, G.S., Fichtinger, G., "Robust fluoroscope tracking fiducial," *Medical Physics* 32 (10): 3185-3198, Oct 2005

[51] Lee, S., Fichtinger, G., Chirikjian, G.S., " Novel Algorithms for Robust Registration of Fiducials in CT and MRI," *Medical Physics*, 29 (8): 1881-1891 AUG 2002

[52] Wolfe, K.C., Mashner, M., Chirikjian, G.S., "Bayesian Fusion on Lie Groups," *Journal of Algebraic Statistics* Vol. 2, No. 1, 2011, 75-97

[53] Kaloutsakis, G., Chirikjian, G.S., "A stochastic self-replicating robot capable of hierarchical assembly," *Robotica*, 29:137–152, 2011.

[54] Chirikjian, G.S., "Information-Theoretic Inequalities on Unimodular Lie Groups," *Journal of Geometric Mechanics*, 2(2):119-158, June 2010.

[55] Kutzer, M.,Brown, C., Scheidt, D., Armand, M., Wolfe, K.,Moses, M., Chirikjian, G., "Reconfigurable Robotic System with Independently Mobile Modules," *Johns Hopkins APL Technical Digest*, 28(3):270–1 (2010)

[56] M.S. Moses, G.S. Chirikjian, "Design of an Electromagnetic Actuator Suitable for Production by Rapid Prototyping," *2011 ASME International Design Engineering Technical Conferences & Computers and Information in Engineering Conference*, paper DETC2011-48602, August 28–31, 2011, Washington, DC, USA.

[57] Chirikjian, G. S., "Information Theory on Lie Groups and Mobile Robotics Applications," *IEEE International Conference on Robotics and Automation*, Anchorage, Alaska, 2751–2757, 2010.

[58] Kutzer, M.D.M., Moses, M.S., Brown, C.Y., Scheidt, D.H., Chirikjian, G.S., Armand, M., "Design of a new independently-mobile reconfigurable modular robot," *IEEE International Conference on Robotics and Automation*, May 2010, pp. 2758–2764.

[59] Wolfe, K.C., Kutzer, M.D.M., Armand, M., Chirikjian, G.S. "Trajectory generation and steering optimization for self-assembly of a modular robotic system," *IEEE International Conference on Robotics and Automation*, May 2010, pp. 4996–5001.